

Characterization of a metastable neon beam extracted from a commercial RF ion source

B. Ohayon and G. Ron*

Racah Institute of Physics, Hebrew University of Jerusalem, Jerusalem 91904, Israel

E. Wählin

Beam Imaging Solutions, 1610 Pace St., Longmont 80504, USA

(Dated: April 4, 2024)

Abstract

We have used a commercial RF ion-source to extract a beam of metastable neon atoms. The source was easily incorporated into our existing system and was operative within a day of installation. The metastable velocity distribution, flux, flow, and efficiency were investigated for different RF powers and pressures, and an optimum was found at a flux density of 2×10^{12} atoms/s/sr. To obtain an accurate measurement of the amount of metastable atoms leaving the source, we insert a Faraday cup in the beam line and quench some of them using a weak 633 nm laser beam. In order to determine how much of the beam was quenched before reaching our detector, we devised a simple model for the quenching transition and investigated it for different laser powers. This detection method can be easily adapted to other noble gas atoms.

I. INTRODUCTION

In 2001, two groups realized the first Bose-Einstein condensate of metastable helium [1, 2]. To excite it to the metastable state, they have both used a high voltage discharge source [3, 4], where atoms are excited to upper states, by running a DC discharge through the expanding atomic beam, which

later decayed to a long-lived metastable state. In recent years, there has been much interest in experiments with ultracold metastable noble gasses (See [5] for a review). Also, advances in the efficiency of production and trapping of metastable noble gasses have enabled spectroscopy and abundance measurements with tiny fractions of rare isotopes. The isotope shift and hyperfine structure of isotopes of argon [6], krypton [7], neon [8] and xenon [9] were measured. Moreover, isotope shift measurements have determined the

* Author to whom correspondence should be addressed. Electronic mail: gron@racah.phys.huji.ac.il

^3He nuclear charge radius [10] and recently those of $^6,^8\text{He}$ [11]. In atomic traps, a novel technique for radio-dating using abundance measurements of noble gas isotopes called Atom Trap Trace Analysis (ATTA) has been introduced with krypton [12], and recently used with argon [13]. Lastly, there is also a growing interest in measurement of cold and trapped short-lived isotopes of the noble gasses neon and helium [14].

These developments have sparked interest in developing efficient metastable sources which are simple to construct, implement and maintain. Exotic sources such as an inverted magnetron pressure gauge [16], and an all optical source [17] have been constructed, but the simplest and most efficient sources today usually rely on an RF discharge [18]. Despite needing much less maintenance than DC discharge sources, home built RF discharge sources degrade over time due to depositions on the discharge tube from sputtering of stainless steel vacuum parts. After experiencing difficulties in continuously operating a home built RF source we decided to acquire a commercial ion source (BIS RFIS-100) and investigate the conditions for efficiently extracting metastable neon atoms from it. In this paper we review our findings.

II. RFIS-100 ION SOURCE

In Fig. 1a, adapted from [15], we show an overview of the source design. neon flows through the gas inlet, is delayed in the ceramic gas isolator to prevent the plasma short-circuiting to ground, and is excited in the alumina discharge chamber (Fig. 1b), where a discharge is created by applying high RF power at 13.56 MHz to a helical resonator copper antenna. The discharge chamber is equipped with an alumina deposition breaker, which serves as to prevent ablated metal particles from forming a conductive coating on the chamber which could shield the discharge from the RF power. A molybdenum beam plate acts as a nozzle which can be easily drilled to different diameters. The source also incorporates a piezoelectric high voltage module to help with ignition of the discharge.

There are normally two modes of operation with RF sources. Namely, capacitively coupled plasma, where electrons accelerated by the RF electric field ionize the gas to cause an avalanche, and inductively coupled plasma (ICP), where the electrons are accelerated by time varying magnetic fields [19]. ICP is initiated at high powers and pressures and is considered desirable in terms of metastable production [20]. The signature of the ICP discharge is the requirement to re-tune the

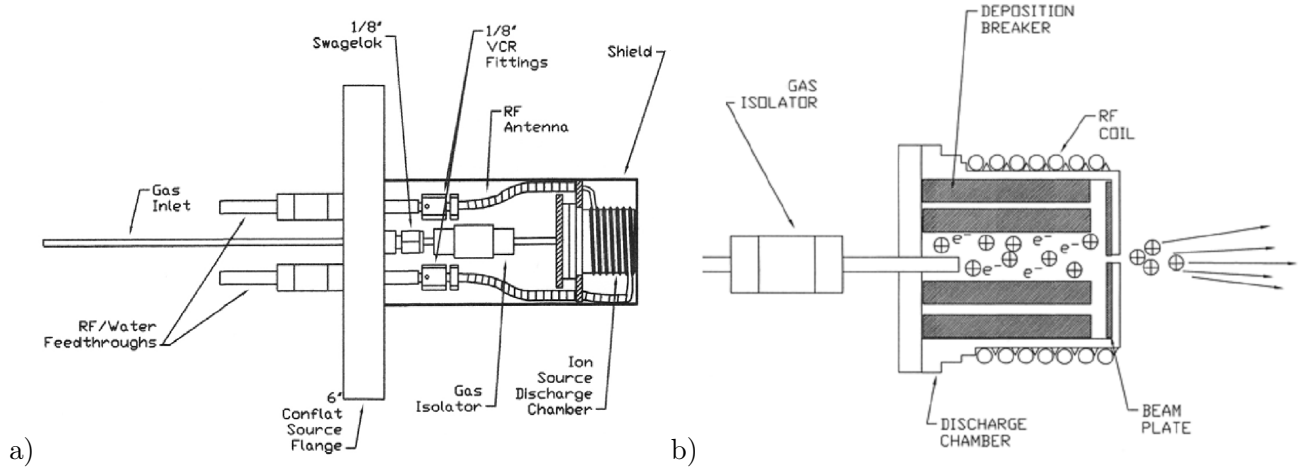


Figure 1. a) RFIS-100 ion source schematics. b) Close up on discharge chamber. Both are adapted from [15].

RF antenna's impedance after the discharge starts. Good impedance matching between the antenna network and the RF power supply (T&C AG 0613 600W) is achieved via two high voltage vacuum variable capacitors that are connected in parallel and in series with the antenna. At virtually all pressures and powers in which neon ignites we observed a drastic change in impedance which indicates the formation of an ICP.

Igniting the plasma is harder than maintaining it, for this reason we usually start at high pressure and high RF power (~ 300 W) and then quickly ramp down the power. Also, it is harder to start the plasma when the source is hot. Even though the hollow antenna is cooled by pumping a high pressure refrigeration fluid (tetrafluoromethane), the 13.56 MHz radiation dissipates significant power in the vacuum parts, and above

250 W, care must be taken. Thus, the power available to the discharge is probably less than the forward power measured by the generator (also reported at [21]). At high pressures of a few 10^{-5} Torr, pure neon lights up easily and plasma can be sustained at powers as low as about 150 W. At low pressures of a few 10^{-6} Torr, plasma can only be sustained at high powers of about 220 W. When mixing a small amount of xenon (Similar to reports by [22]), the plasma ignites at virtually all powers and pressures.

III. LIGHT INDUCED QUENCHING OF METASTABLE NEON

The steady-state scattering rate of classical radiation by a two level system with natural linewidth Γ is [23]

$$r(\vec{v}) = \frac{s_0/2}{1 + s_0 + (2\delta(\vec{v})/\Gamma)^2}, \quad (1)$$

where $s_0 = I_l/I_s$ is the saturation parameter, I_l is the laser intensity, and I_s the saturation intensity. The detuning is given by

$$\delta(\vec{v}) = \delta_0 - \vec{k} \cdot \vec{v} \quad (2)$$

where δ_0 is the difference between the laser and the atomic transition frequency, and $\vec{k} \cdot \vec{v}$ the Doppler detuning, caused by the relative velocity of the light and atom.

Noble gasses possess a long lived metastable state which forms such a two-level system [5]. With neon, the cycling transition is between the levels $^3P_2 - ^3D_3$, as shown in Fig. 2. Its wavelength in air is 640.2 nm. It has a linewidth of $\Gamma = 8.2(2\pi)$ MHz, or, using eq. 2, $\sigma_\Gamma = \Gamma/k = 5.2$ m/s in units of velocity. Another transition of interest is $^3P_2 - ^3D_2$ which has a wavelength of 633.4 nm [24]. It is not a closed transition, since the 3D_2 state can decay via a dipole transition to the 3P_1 and 1P_1 states (which decay immediately to the ground state) as well as to 3P_2 . Thus a laser tuned to this wavelength can deplete the population in the 3P_2 state; this process is also called *quenching*. The states of interest, and the relevant wavelengths are presented in Fig. 2.

When a metastable beam encounters a laser beam tuned to the quenching transition,

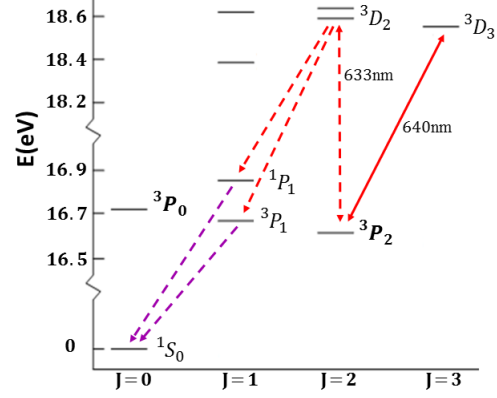


Figure 2. Relevant transition lines of neon [25].

The metastable levels $^3P_{0,2}$ are indicated in bold. Upward facing arrows represent transitions coupled by our lasers, with the wavelength indicated. Downward facing arrows represent emission. The solid line represents the cycling transition and the broken lines represent the quenching route.

the atoms have a chance of absorbing photons and deexciting from the metastable state. The longer an atom spends inside the quench beam, and the stronger the laser, the chances of its survival decrease exponentially. For a transverse laser locked to the quenching transition, the detuning from the atomic transition is governed by the atom's transverse velocity (eq. 2). We thus model, using eq. 1, this average survival rate of a metastable atom, with v_r and v_z the transverse and longitudinal velocities, which travels through a weak transverse quenching beam can be written as

$$f_Q(v_z, v_r) = \exp\left(-\frac{v_q}{v_z} \frac{1}{1 + (2v_r/\sigma_q)^2}\right). \quad (3)$$

Where v_q is the effective intensity of the quench laser, and σ_q is an effective transition linewidth, both in units of velocity. Since our source incorporates a discharge chamber with a small aperture (Fig. 1), the emerging beam is assumed to have an effusive velocity distribution [26]:

$$f_B(v_r, v_z) = \frac{9}{2} \frac{v_z^3}{v_{mp}^4} \exp\left(-\frac{3}{2} \frac{v_z^2}{v_{mp}^2}\right) \times \frac{1}{\sigma_r^2} \exp\left(-\frac{v_r^2}{2\sigma_r^2}\right), \quad (4)$$

which is cylindrically normalized such that $\int_0^\infty \int_0^\infty f_B(v_r, v_z) v_r dv_r dv_z = 1$. v_{mp} is the most probable velocity, and σ_r the transverse rms velocity. The total velocity distribution of an atomic beam which passed a transverse laser tuned to the quenching transition is thus

$$f_{tot}(v_r, v_z) = f_B(v_r, v_z) f_Q(v_z, v_r).$$

Adding a weak probe beam tuned to the cycling transition and collecting the fluorescence using a photomultiplier tube (PMT), we measure a signal proportional to

$$F(v_r) = \int_0^\infty f_{tot}(v_z, v_r) dv_z \quad (5)$$

for a transverse probe beam, and to

$$F(v_z) = \int_0^\infty f_{tot}(v_z, v_r) v_r dv_r \quad (6)$$

for a longitudinal probe.

To investigate the working conditions of the source, we use a weak transverse beam which probes the cycling transition and record the PMT signal for different RF powers and neon pressures. The scan voltage to frequency calibration was accomplished by conducting a wide scan and observing the isotope shift on a saturated absorption setup [27]. Since the fluorescence is visible to the naked eye, we noticed a slight fluorescence inside the entire source chamber which is unrelated to the atomic beam. Since we work with high RF power, we conclude that some of the background gas is also excited. This means that our PMT signal is comprised of a narrow atomic beam signal atop a wider background signal. This assumption is validated when we use the quenching beam.

In Fig 3, we show the results obtained from fitting the PMT signal to a double Gaussian for different working conditions. Even though the atomic flux increases with pressure, high chamber pressure tend to quench the metastable beam through collisional deexcitations inside as well as outside of the source [28]. The optimum flux is at a chamber pressure of about 5×10^{-6} Torr and does not change much with RF power, which has to be above 200 W to sustain plasma at such low pressures. Also, a small increase of the transverse velocity is observed at high

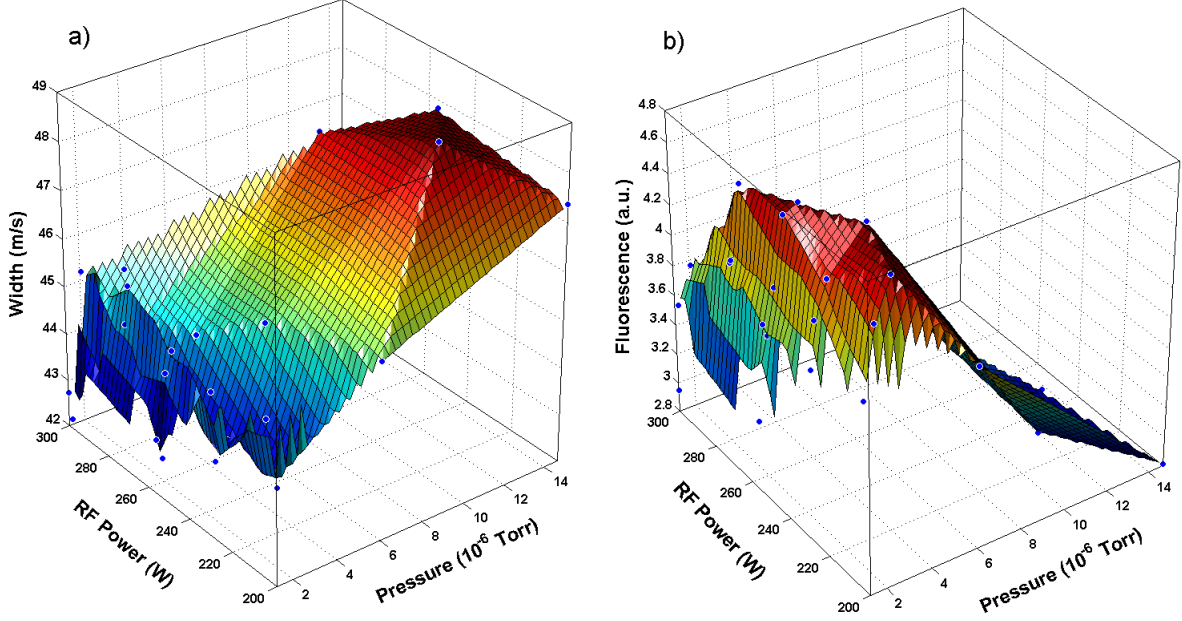


Figure 3. a) Transverse velocity width as a function RF power and chamber pressure. b) Total fluorescence as a function RF power and chamber pressure.

pressures, the transverse rms velocity at the desired pressure is $\sigma_r = 45$ m/s.

To investigate the properties of the quenching transition, we add a large transverse 633 nm beam immediately after the source aperture, which quenches some of the metastable atoms before they reach the light collection region. For a transverse probe beam, we observe that the quenching beam affects the metastable atomic beam signal without affecting the background signal. We thus fit to a wide Gaussian plus transverse quenching (eq. 5). A typical fit, as well as the underlying fit with the background subtracted, is shown in Fig. 4a. The same was done with a longitudinal probe beam and fit

to eq. 6 and is shown in Fig. 4b. We recorded and fit the transverse and longitudinal quenched fluorescence signal for different quench laser powers. The results are shown in Fig. 5. As modeled in eq. 3, the effective quench laser power v_q at low quench powers is linear with laser power and gives similar results for both the transverse and longitudinal probes. Also, the effective transition linewidth σ_q is constant over a wide range of quench laser power.

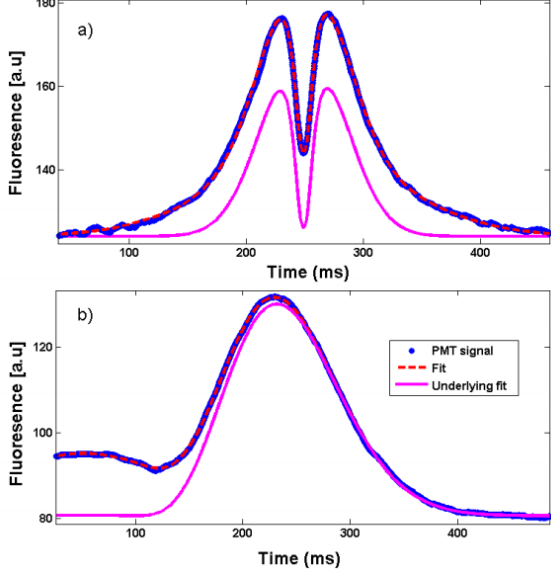


Figure 4. Example of fluorescence quenching fit at 3 mW laser power. a) Transverse probe scope signal, fitted to eq. 5 (dashed line). b) Longitudinal probe signal, fitted to eq. 6. Solid lines are the fits with the background Gaussian subtracted.

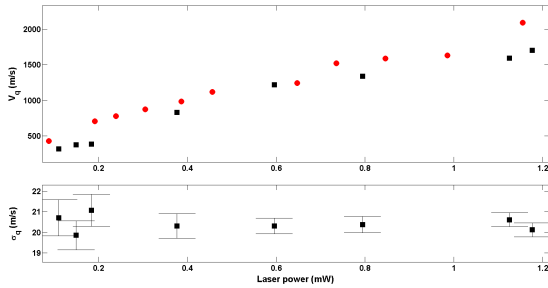


Figure 5. (Top) Effective quench laser power v_q for transverse (squares) and longitudinal (circles) probing. Markers are larger than the error bars. (Bottom) Effective transition linewidth σ_q for transverse probing.

IV. METASTABLE DETECTION USING A FARADAY-CUP

Schemes for detecting metastable atoms usually rely on their long lifetime and large stored energy [29]. When metastable atoms collide with most surfaces, they immediately ionize them. If the surface is a conductor, a measurement of the ionization current can be used to determine the flux of metastable atoms in a beam.

In neon, the metastable states have approximately $E^* = 16$ eV of internal energy, and the ionization energy is $E^+ \sim 22$ eV. When impacting on a metal surface with work function Φ , which for stainless steel is under 4.7 eV [29], two energetic conditions are met: $E^* > \Phi$ and $E^+ \geq 2\Phi$, which enable two ionization processes by an exchange of electrons between the metal and the atom [30]. The absolute metastable flux F can be determined through [31]

$$I = e\gamma F\Delta Y, \quad (7)$$

where I is the ionization current, e is the fundamental charge, $\gamma = 0.61$ the emission coefficient for stainless steel impacted by Ne^* [31], and ΔY is the fraction of atoms detected.

To implement this detection scheme we use a design similar to that of [32], for which a stainless steel detector plate is mounted,

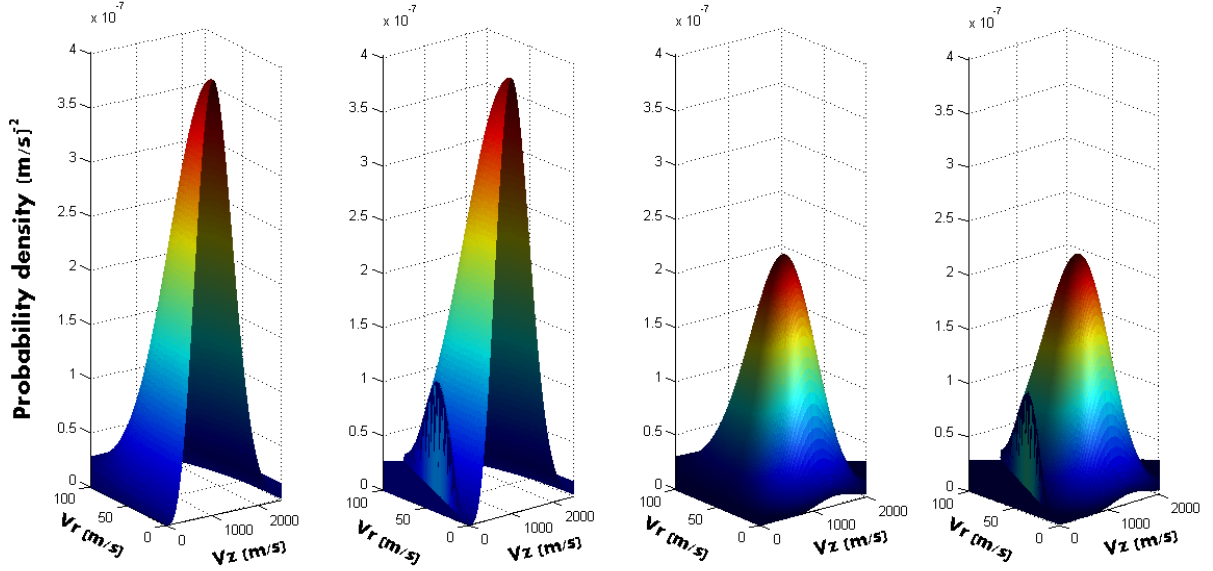


Figure 6. Probability density of transverse and longitudinal velocity distributions. Left to right: Distribution of metastables leaving the source (100%), Metastables that reach the Faraday-cup (84%), Metastables left after crossing the quench laser beam (79%), Metastables that reach the cup after crossing quench beam (64%)

along with an electron collecting cathode, along the beam line. Upon operating the source, a large and noisy negative current ($5\mu\text{A}$) was measured. To stabilize the current, a transverse magnetic field (50 Gauss) was introduced by mounting a coil on the vacuum window of the source chamber and flowing a large current ($\sim 10\text{ A}$). The field deflects fast electrons and ions before they reach the cup. To establish how much of the current left results from atoms in the 3P_2 state only, we measure it again with the population depleted by quenching it using the quench beam and subtract the results. This method is similar to that used by [33] for

neon, but since we did not need to quench all of the atomic beam, we could use a quench laser two orders of magnitude weaker.

Based on the transverse and longitudinal velocity distributions, and the distance and radius of the cup, we calculate the fraction of metastables that reach the cup and arrive at the fraction $Y_0 = 0.84$. We now simulate the amount of metastables reaching the cup when the quenching laser is on and at maximal power using the parameters from Fig. 4, and arrive at the fraction $Y_1 = 0.64$. The fraction of metastables which reach the cup and are quenched by the laser is thus $\Delta Y = Y_0 - Y_1 = 0.20$.

The maximal difference current obtained using the Faraday cup was $I = 8 \text{ nA}$, using eq. 7 we calculate that the metastable flow is $4.2 \times 10^{11} \text{ Ne}^*/\text{s}$. The average flux density in forward direction is then $2.3 \times 10^{12} \text{ Ne}^*/\text{s/sr}$. The flow and flux depend strongly on the pumping speed, our source was pumped by two turbo-molecular pumps which has a combined pumping speed of 400 l/s. The total flow was measured using a flow meter to be 1.4 sccm or $6.5 \times 10^{17} \text{ Ne/s}$. Which yields an efficiency of about 10^{-6} . This is the efficiency at maximum metastable flux. By operating the source with xenon, and mixing small amounts of neon ($< 10^{-6} \text{ Torr}$), a factor of 2-3 is obtained with the efficiency and 10 – 20 of the flux is lost.

V. SUMMARY AND OUTLOOK

We have devised a simple, *ad hoc* model to investigate the amount of metastable neon atoms which are left after crossing a laser beam tuned to a quenching transition. This model was used to investigate how much of

the ionization current in a Faraday-cup resulted from atoms in a specific metastable state and so determine the metastable flux density. Combined with spectroscopic measurements of the velocity distribution, and a measurement of the atomic flow, a complete picture of our source was obtained. Since the energy levels of other noble gasses are similar, this detection method can be readily used in existing metastable systems. The simplicity of incorporating, operating, and maintaining a commercial source might make it a choice for future industrial applications such as metastable atom lithography [34].

VI. ACKNOWLEDGMENTS

The authors thank M. Oberthaler and the Synthetic Quantum Systems Group at the Kirchhoff Institute for Physics at the University of Heidelberg. This work was supported by the Israeli Science Foundation under ISF grant 177/11. Ben Ohayon is supported by the Hoffman Leadership and Responsibility fund.

-
- | | |
|--|--|
| <p>[1] A. Robert, O. Sirjean, A. Browaeys, J. Poupard, S. Nowak, D. Boiron, C. I. Westbrook, and A. Aspect, <i>Science</i> 292, 461 (2001).</p> | <p>[2] F. Pereira Dos Santos, J. Léonard, J. Wang, C. J. Barrelet, F. Perales, E. Rasel, C. S. Unnikrishnan, M. Leduc, and C. Cohen-Tannoudji, <i>Phys. Rev. Lett.</i> 86, 3459 (2001).</p> |
|--|--|

-
- [3] A. Browaeys, J. Poupard, A. Robert, S. Nowak, W. Rooijakkers, E. Arimondo, L. Marcassa, D. Boiron, C. Westbrook, and A. Aspect, *The European Physical Journal D* **8**, 199 (2000), ISSN 1434-6060.
- [4] n. F. Pereira Dos Santos, F. Perales, J. LÃ©onard, A. Sinatra, J. Wang, F. S. Pavone, E. Rasel, C. S. Unnikrishnan, and M. Leduc, *The European Physical Journal Applied Physics* **14**, 69 (2001), ISSN 1286-0050.
- [5] W. Vassen, C. Cohen-Tannoudji, M. Leduc, D. Boiron, C. I. Westbrook, A. Truscott, K. Baldwin, G. Birkel, P. Cancio, and M. Trippenbach, *Rev. Mod. Phys.* **84**, 175 (2012).
- [6] K. Blaum, W. Geithner, J. Lassen, P. Lievens, K. Marinova, and R. Neugart, *Nuclear Physics A* **799**, 30 (2008), ISSN 0375-9474.
- [7] B. D. Cannon and G. R. Janik, *Phys. Rev. A* **42**, 397 (1990).
- [8] T. Feldker, J. Schutz, H. John, and G. Birkel, *The European Physical Journal D* **65**, 257 (2011), ISSN 1434-6060.
- [9] M. Walhout, H. J. L. Megens, A. Witte, and S. L. Rolston, *Phys. Rev. A* **48**, R879 (1993).
- [10] P. Zhao, J. R. Lawall, and F. M. Pipkin, *Phys. Rev. Lett.* **66**, 592 (1991).
- [11] Z.-T. Lu, P. Mueller, G. W. F. Drake, W. Nörtershäuser, S. C. Pieper, and Z.-C. Yan, *Rev. Mod. Phys.* **85**, 1383 (2013).
- [12] C. Y. Chen, Y. M. Li, K. Bailey, T. P. O'Connor, L. Young, and Z.-T. Lu, *Science* **286**, 1139 (1999).
- [13] T. Reichel, A. Kersting, F. Ritterbusch, S. Ebser, K. Bender, R. Purtschert, M. Oberthaler, and W. Aeschbach-Hertig, in *EGU General Assembly Conference Abstracts* (2013), vol. 15, p. 10901.
- [14] J. A. Behr and A. Gorelov, *Journal of Physics G: Nuclear and Particle Physics* **41**, 114005 (2014).
- [15] E. Wahlin, *Model RFIS-100 RF ion source User's Manual*, Beam Imaging Solutions (2011).
- [16] M. H. L. van der Velden, H. Batelaan, E. te Sligte, H. C. W. Beijerinck, and E. J. D. Vredenburg, *Review of Scientific Instruments* **75** (2004).
- [17] H. Daerr, M. Kohler, P. Sahling, S. Tippenhauer, A. Arabi-Hashemi, C. Becker, K. Sengstock, and M. B. Kalinowski, *Review of Scientific Instruments* **82**, 073106 (2011).
- [18] C. Y. Chen, K. Bailey, Y. M. Li, T. P. O'Connor, Z.-T. Lu, X. Du, L. Young, and G. Winkler, *Review of Scientific Instruments* **72**, 271 (2001).

- [19] H. Conrads and M. Schmidt, Plasma Sources Science and Technology **9**, 441 (2000).
- [20] F. Ritterbusch, Ph.D. thesis, Kirchhoff Institute for Physics (2009).
- [21] J. Welte, Ph.D. thesis, Ruperto-Carola-University of Heidelberg (2011).
- [22] I. A. Sulai, Ph.D. thesis, University of Chicago (2011).
- [23] W. D. Phillips, J. V. Prodan, and H. J. Metcalf, J. Opt. Soc. Am. B **2**, 1751 (1985).
- [24] Y. Ralchenko, A. E. Kramida, J. Reader, and N. A. S. D. Team, *NIST Atomic Spectra Database (version 3.1.5)* (2008).
- [25] A. Kramida, Yu. Ralchenko, J. Reader, and NIST ASD Team.
- [26] H. Pauly, *Atom, Molecule, and Cluster Beams I: Basic Theory, Production and Detection of Thermal Energy Beams* (Springer, 2000).
- [27] B. Lubotzky, Master's thesis, Hebrew University of Jerusalem (2013).
- [28] J. Welte, F. Ritterbusch, I. Steinke, M. Henrich, W. Aeschbach-Hertig, and M. K. Oberthaler, New Journal of Physics **12**, 065031 (2010).
- [29] H. Hotop, in *Atomic, Molecular, and Optical Physics: Atoms and Molecules*, edited by F. Dunning and R. G. Hulet (Academic Press, 1996), vol. 29, Part B, pp. 191 – 215.
- [30] A. Cobas and W. E. Lamb, Phys. Rev. **65**, 327 (1944).
- [31] F. B. Dunning, R. D. Rundel, and R. F. Stebbings, Review of Scientific Instruments **46** (1975).
- [32] J. P. Ashmore, Ph.D. thesis, Griffith University (2005).
- [33] J. A. Brand, J. E. Furst, T. J. Gay, and L. D. Scheerer, Review of Scientific Instruments **63**, 163 (1992).
- [34] C. S. Allred, J. Reeves, C. Corder, and H. Metcalf, Journal of Applied Physics **107**, 033116 (2010).